Applied Sciences, Computing and Energy, 2025, 2(2), 299-322

Computational Design of Pyridyl-Benzaldehyde Derivatives as Eco-Friendly Corrosion Inhibitors: A DFT-Based Study

Babatunde T. Ogunyemi*

Received: 18 January 2025/Accepted: 28 March 2025/Published: 04 April 2025

Abstract ***:****In modern times, the corrosion industries are intensively determined in the exploitation of ecofriendly inhibitors to substitute existing ones that are relatively toxic. Large number of organic compounds has been investigated as corrosion inhibitors. However, only a few Pyridyl derivatives have been investigated as corrosion inhibitors. This study employs Density Functional Theory (DFT) at the B3LYP/6-31G(d) level to evaluate the corrosion inhibition potential of eleven pyridyl- benzaldehyde derivatives. Quantum chemical parameters, including frontier molecular orbitals (HOMO, LUMO), global reactivity descriptors (electronegativity, hardness, softness), and local reactivity indices (Fukui functions), were computed to elucidate the adsorption mechanisms and inhibition efficiency. Results reveal that structural modifications, particularly the position of nitrogen in the pyridine ring and methoxy substituents on benzaldehyde, critically influence electronic properties. Molecules 9, 10, and 11 exhibited superior corrosion inhibition potential due to their high HOMO energies (-5.18 to -5.06 eV), low LUMO energies (-1.62 to -1.36 eV), and favorable electron transfer capabilities (ΔN = -1.075 to -1.123). Fukui indices identified nitrogen and oxygen atoms as active sites for donor-acceptor interactions with metal surfaces. Additionally, dipole moments (5.08–5.80 Debye) and molecular volume/area trends further corroborated enhanced adsorption for these derivatives. This computational approach provides a predictive framework for designing eco-friendly, high-performance corrosion inhibitors, emphasizing the role of heteroatom positioning and substituent effects in optimizing molecular reactivity.*

Keywords: *Corrosion inhibition, Density Functional Theory (DFT), Pyridyl derivatives, Quantum chemical parameters*

Babatunde T. Ogunyemi*
Department of Chemistry, Federal University Otuoke, Bayelsa State, Nigeria
Email: ogunyemibt@fuotuoke.edu.ng
Orcid id:0000-0002-3634-488X

1.0 Introduction

Corrosion is a natural and inevitable process that affects virtually every sector reliant on metals, including transportation, construction, manufacturing, and energy (Roberge, 2008). It refers to the gradual degradation of materials—particularly metals—through chemical interactions with their environment. Beyond aesthetic deterioration, corrosion presents a profound structural risk that compromises functionality, safety, and the lifespan of materials (Koch et al., 2016). Catastrophic failures of infrastructure such as pipelines, industrial equipment, and bridges have often been traced to unchecked corrosion. Consequently, the development of effective, non-toxic, and eco-friendly corrosion inhibitors has become a central focus in materials science and engineering, aimed at enhancing industrial sustainability and reducing ecological impact (Verma et al., 2020; Ogunyemi et al., 2020).

Corrosion typically proceeds via electrochemical processes, especially in aqueous environments. Metals like iron and steel undergo oxidation at the anode, releasing electrons that travel to the cathode, where reduction reactions occur—resulting in corrosion products such as rust (iron oxide). The presence of aggressive ions like chloride (Cl^-), common in marine environments, accelerates these reactions. While protective coatings and cathodic protection are conventional countermeasures (Tezdogan and Demirel, 2014), corrosion inhibitors—compounds that reduce the corrosion rate when introduced into the corrosive environment—are among the most versatile and cost-effective solutions (Ogunyemi et al., 2020; Shwetha et al., 2024).

Organic compounds containing heteroatoms such as nitrogen, oxygen, and sulfur have shown great promise as corrosion inhibitors (Brycki et al., 2018; Shwetha et al., 2024; Chandra, 2023). These compounds adsorb onto metal surfaces to form protective layers that hinder the access of corrosive species. Lone pair electrons or π-electrons in these molecules often interact strongly with active sites on the metal (Mahmoud et al., 2024; Afshari et al., 2023; Setti et al., 2025; Baharin et al., 2024). Pyridine-based derivatives, in particular, are of great interest due to the coordinating ability of the nitrogen atom, which enhances their binding affinity to metal surfaces. Their effectiveness is largely governed by molecular structure, which influences adsorption behavior and inhibitor film stability (Espinoza-Vázquez et al., 2019; Okewale and Adebayo, 2020).

Modifying the molecular structure of these organic compounds—such as changing the position of functional groups or introducing new substituents—is a well-established strategy for improving inhibition efficiency (Liu et al., 2024; Al-Baghdadia et al., 2025). For heterocyclic compounds like pyridine, repositioning the nitrogen atom or introducing electron-donating groups (e.g., methoxy substituents) can significantly alter electronic distributions, thereby influencing how the molecule interacts with metal surfaces (Chaouiki et al., 2022; Malik et al., 2025). However, despite the extensive research on organic corrosion inhibitors, only a limited number of pyridyl derivatives—particularly pyridyl-benzaldehyde compounds—have been studied for corrosion inhibition. This represents a significant gap in knowledge, especially regarding how structural modifications like nitrogen repositioning and methoxy substitution influence inhibition performance.

To address this gap, the present study investigates the corrosion inhibition properties of eleven pyridyl-benzaldehyde derivatives using Density Functional Theory (DFT). Specifically, it evaluates how repositioning of the nitrogen atom within the pyridine ring and variation in methoxy substitution on the benzaldehyde moiety affect the electronic structure, adsorption behavior, and overall inhibition efficiency of the molecules.

Computational methods such as DFT and Monte Carlo simulations have become indispensable tools in this domain. They enable accurate evaluation of quantum chemical parameters and prediction of adsorption behavior and inhibition performance (Lgaz et al., 2025; Ayuba et al., 2023). DFT, in particular, offers deep insights into molecular reactivity by computing electronic structure descriptors such as frontier molecular orbitals and local reactivity indices (Obot et al., 2015). Monte Carlo simulations complement these calculations by modeling the dynamic interaction of inhibitor molecules with metal surfaces, identifying energetically favorable adsorption configurations. By combining these techniques, this study seeks to establish a robust theoretical framework for the rational design of eco-friendly, high-performance corrosion inhibitors. The outcomes have broad implications for materials science, engineering applications, and sustainable industrial practices.

2.0 Materials and Methods

Molecular modeling techniques have emerged as a formidable alternative for interpreting experimental data, especially when it comes to predicting the properties of new materials that align with industrial needs. In this work, all calculation was executed using quantum chemical methods within version 2.4 of the Spartan 14 package, focusing on an isolated gaseous system maintained at a temperature of 298.15K and a pressure of 1 atmosphere. Ground-state geometry optimization and energy calculations for the ten Pyridyl-Benzaldehyde Derivatives of were performed using DFT/B3LYP (Becke et al., 1993; Lee et al., 1988) with the 6-31G(d) basis set (Yang et al., 1998). During optimization, all bond angles, dihedral angles, and bond lengths were unconstrained, ensuring that real vibrational frequencies were achieved. The energy levels of the molecular orbitals, specifically E_{HOMO} and E_{LUMO}, were computed to identify key adsorption sites. These molecular frontier orbitals (HOMO and LUMO) are instrumental in predicting how the studied organic inhibitors interact with metal surfaces.

Moreover, the ionization potential (IP) and electron affinity (EA) of all the studied inhibitors were derived from the HOMO and LUMO energies using Koopman's theorem (Pearson et al., 1988), as shown in the following equations:

$$IP = -E_{HOMO} \qquad (1)$$

$$EA = -E_{LUMO} \qquad (2)$$

The absolute hardness and electronegativity (χ) values of the studied molecules were calculated using the formular below.

$$\eta = \left(\frac{\delta\varepsilon^2}{\delta N^2}\right)_{v(r)} = \frac{E_{LUMO} + E_{HOMO}}{2} = \frac{IP - EA}{2} \qquad (3)$$

$$\chi = -\mu = \left(\frac{\delta\varepsilon}{\delta N}\right)_{v(r)} = -\frac{E_{LUMO} + E_{HOMO}}{2} = \frac{IP + EA}{2} \qquad (4)$$

The softness (S), which is the inverse of hardness, was determined through:

$$S = \frac{1}{\eta} \qquad (5)$$

These quantum parameters (hardness electronegativity, and softness) are critical in assessing the chemical reactivity of the organic inhibitors.

When a metal makes contact with an organic molecule, electrons flow between the two systems until their chemical potentials align. The number of transferred electrons (ΔN) was calculated as reported in the work of Parr et al., (1983):

$$\Delta N = \frac{\chi_{Fe} - \chi_{inh}}{2(\eta_{Fe} + \eta_{inh})} \qquad (6)$$

where χ_{Fe} and χ_{inh} represent the absolute electronegativities of iron (Fe) and organic inhibitor respectively. while η_{Fe} and η_{inh} represent their hardness. For iron, theoretical values of $\chi_{Fe} = 7$ eV/mole and $\eta_{Fe} = 0\ eV/mole$ (Ogunyemi, *et al.*, 2020) were u employed to estimate the electron transfer**.**

The back-donation charges which is a crucial parameter for understanding charge redistribution, was calculated using equation 2 given below,

$$\Delta E_{(Back-donation)} = \frac{\mu}{4} \qquad (6b)$$

Additionally, the electrophilicity index (ω) of each molecular inhibitors was evaluated through the following equation (Parr et al., 1999):

$$\omega = \frac{\mu^2}{2\eta} \qquad (7)$$

A lower μ and ω indicate a more reactive nucleophile, while higher values suggest an active electrophile.

The Pyridyl-Benzaldehyde Derivatives (Table 1) were theoretically investigated for their corrosion inhibition efficiency using DFT/B3LYP/6-31G*. Table 1 displayed the molecular structures, optimized structures and the names of each of the studied inhibitors. The geometric structures of the Pyridyl-Benzaldehyde Derivatives presented shows that nitrogen is present at different position of the pyrindene and methoxy group at different position on benzaldehyde structure.

Table 1: Structures and names Pyridyl Derivatives of Benzaldehyde studied

S/N	**Molecular structure of the Pyridyl Derivatives of Benzaldehyde**	**Optimized structures**	**Name**
1	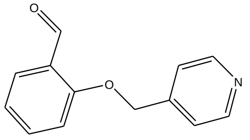	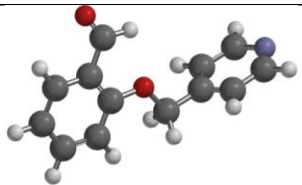	2-[(pyridine-4-yl)methoxy]benzaldehyde
2	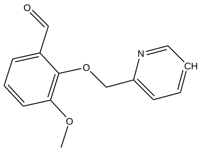	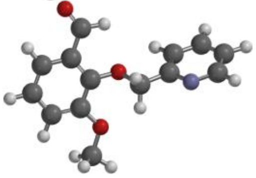	2-((pyridine-2-yl)methoxy)-3-methoxylbenzaldehyde
3	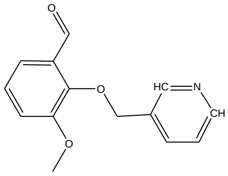	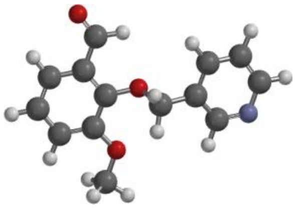	2-[(pyridine-3-yl)methoxy) -3-methoxybenzaldehyde
4	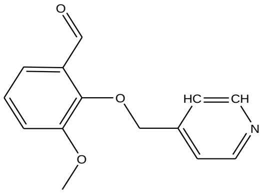	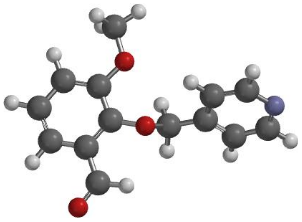	2-[(pyridine-4-yl)methoxy) -3-methoxybenzaldehyde
5	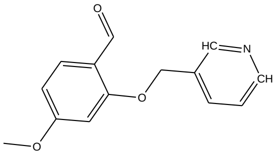	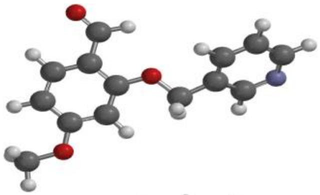	2-[(pyridine-3-yl)methoxy) -4-methoxybenzaldehyde
6	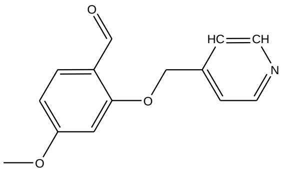	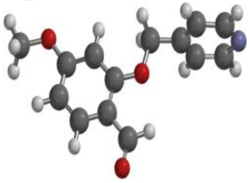	2-[(pyridine-4-yl)methoxy) -4-methoxybenzaldehyde
7	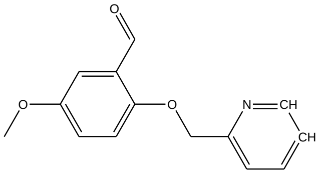	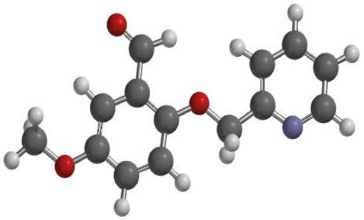	2-[(pyridine-2-yl)methoxy) -5-methoxybenzaldehyde

8	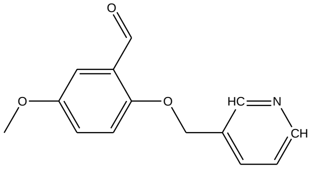	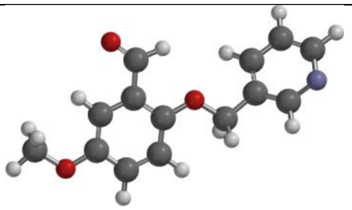	2-[(pyridine-3-yl)methoxy) -5-methoxybenzaldehyde
9	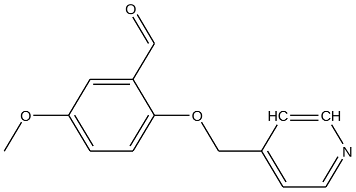	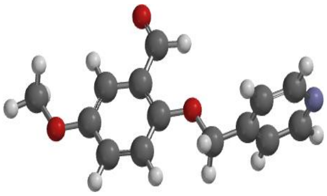	2-[(pyridine-4-yl)methoxy) -5-methoxybenzaldehyde
10	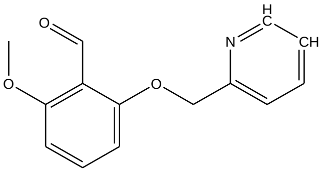	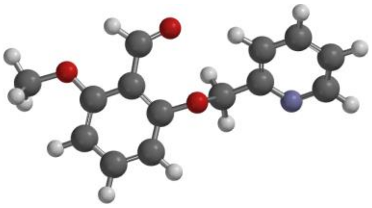	2-[(pyridine-2-yl)methoxy) -6-methoxybenzaldehyde
11	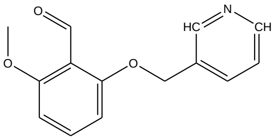	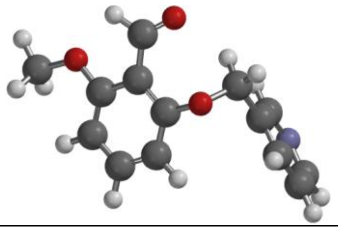	2-[(pyridine-3-yl)methoxy) -6-methoxybenzaldehyde

3.0. Results and Discussion

3.1 Quantum Parameters

Tables 2 and 3 present the calculated quantum chemical parameters for the eleven investigated molecules, divided into two groups for clarity: Molecules 1 to 6 and Molecules 7 to 11, respectively. These parameters were derived using Density Functional Theory (DFT) calculations and include important descriptors such as the energies of the Highest Occupied Molecular Orbital (EHOMO) and the Lowest Unoccupied Molecular Orbital (ELUMO), energy gap (ΔE), ionization potential (I), electron affinity (A), electronegativity (χ), global hardness (η), global softness (S), electrophilicity index (ω), dipole moment (μ), and polarizability (α). These descriptors are critical in assessing the chemical reactivity and potential inhibitory behavior of the molecules.

The HOMO energy indicates the molecule's ability to donate electrons, while the LUMO energy reflects its ability to accept electrons. A lower energy gap generally corresponds to higher chemical reactivity and better interaction with the metal surface. Other parameters such as electronegativity, hardness, and softness provide insight into the molecule's stability and polarizability, which influence its adsorption behavior. The electrophilicity index reflects the stabilization energy upon gaining electrons, and the dipole moment and polarizability offer information on molecular orientation and electron cloud distortion in an external field, which are relevant to the molecule's performance in corrosion inhibition. Together, these data provide a comprehensive basis for evaluating the suitability of the molecules as corrosion inhibitors.

The results and interpretation of the computational analysis for the eleven molecules are discussed in terms of their energy profiles, electronic properties, solvation tendencies, and potential reactivity.

Table 2: Calculated Quantum chemical parameters for molecules 1 to 6

Molecular Parameters	**Molecule 1**	**Molecule 2**	**Molecule 3**	**Molecule 4**	**Molecule 5**	**Molecule 6**
Energy	-2460.77	-2115.69	-2460.77	-4574.46	-2040.49	-5034.05
E$_{solv}$ (kJ/mol)	-44.1	-49.59	-45.41	-47.06	-43.65	-43.86
E$_{HOMO}$ (eV)	-5.88	-5.56	-5.88	-5.89	-5.72	-5.97
E$_{LUMO}$ (eV)	-1.76	-1.35	-1.81	-1.83	-1.53	-1.88
DM (debye)	3.24	4.33	2.71	2.68	3.93	1.51
ΔE (eV)	4.12	4.21	4.07	4.06	4.19	4.09
Area	426.87	441.02	428.87	433.58	433.22	446.94
V	413.01	426.43	413.3	417.77	417.9	431.11
ovality	1.59	1.61	1.6	1.6	1.6	1.62
PSA	29.145	36.125	29.257	29.207	29.226	29.004
LogP	2.24	1.4	2.24	2.51	2.55	2.38
polarizability	73.9	74.97	73.94	74.3	74.28	75.38
IP	5.88	5.56	5.88	5.89	5.72	5.97
EA	1.76	1.35	1.81	1.83	1.53	1.88
S(eV^{-1})	0.485	0.475	0.491	0.493	0.477	0.489
η (eV)	2.06	2.105	2.035	2.03	2.095	2.045
X	3.82	3.455	3.845	3.86	3.625	3.925
ΔN	-0.74346	-0.92402	-0.70416	-0.69883	-0.84207	-0.60764
ΔE(Back-Donation)	-0.33	-0.15375	-0.39625	-0.40125	-0.22375	-0.5575
w	-0.22806	-0.05474	-0.32669	-0.33368	-0.11049	-0.63349

Molecule 1 exhibited a relatively low energy value of -2460.77, suggesting good structural stability. Its solvation energy of -44.1 kJ/mol indicates a moderate affinity for aqueous media. With a HOMO-LUMO energy gap of 4.12 eV, it is moderately reactive, while its dipole moment of 3.24 D reflects a balanced polarity. The logP value of 2.24 suggests favorable lipophilicity for membrane permeability, and its electronegativity of 3.82 reveals a strong electron-withdrawing nature. The softness value of 0.485 eV^{-1} and ΔN of -0.743 indicate that Molecule 1 can accept electrons, marking it as electrophilic.

In comparison, Molecule 2 showed slightly lower stability with an energy of -2115.69 but demonstrated better aqueous solvation at -49.59 kJ/mol. It has a slightly larger energy gap of 4.21 eV, indicating it is less reactive than Molecule 1. Its dipole moment is higher at 4.33 D, suggesting increased polarity, and with a logP of 1.4, it is more hydrophilic. Its electronegativity, at 3.455, is slightly lower, and the electron back-donation energy is mildly negative, pointing to a modest ability to share electrons.

Molecule 3 shared the same total energy as Molecule 1 but had a slightly smaller HOMO-LUMO gap of 4.07 eV, implying greater reactivity. Its dipole moment was lower at 2.71 D, denoting reduced polarity. Electronegativity remained comparable at 3.845, while the electrophilicity index ω was moderately negative, suggesting it maintains an electrophilic character.

Molecule 4 displayed the highest stability among the first four molecules, with an energy of -4574.46. The energy gap of 4.06 eV points to reactivity similar to the others. Its dipole moment was relatively low at 2.68 D, suggesting limited polarity, while an electronegativity of 3.86 and a ΔN of -0.6988 further support its electron-accepting nature. The electrophilicity index was strongly negative, confirming its tendency to act as an electrophile.

Molecule 5, although less stable at -2040.49, had a high dipole moment of 3.93 D and a logP of 2.55, which could enhance its bioavailability and membrane permeation. Its energy gap of 4.19 eV suggests it is slightly less reactive. It also had a moderate electronegativity of 3.625 and an appreciable electron-accepting capacity with a ΔN of -0.842.

Molecule 6 demonstrated the highest overall stability with an energy of -5034.05 and a moderate energy gap of 4.09 eV. Its dipole moment was notably low at 1.51 D, indicating low polarity. A logP of 2.38 suggests moderate lipophilicity, and its electrophilicity index was the most negative among all, reflecting a strong tendency to act as an electrophile.

Table 2: Calculated Quantum chemical parameters for molecules 7 to 11

Molecular Parameters	Molecule 7	Molecule 8	Molecule 9	Molecule 10	Molecule 11
Energy	-2500.09	-2575.27	-4248.83	-1714.86	-1790.07
E_{solv} (kJ/mol)	-40.79	-47.42	-41.64	-49.45	-55.98
E_{HOMO} (eV)	-5.8	-5.65	-5.18	-5.09	-5.06
E_{LUMO} (eV)	-1.57	-1.45	-1.42	-1.37	-1.36
DM (debye)	3.5	3.87	5.8	5.48	5.08
ΔE (eV)	4.23	4.20	3.76	3.72	3.71
Area (	446.78	456.52	469.75	469.23	478.9
V	431.25	440.07	453.48	453.52	462.31
ovality	1.62	1.63	1.65	1.64	1.66
PSA	29.048	36.007	30.416	30.494	37.446
LogP	2.42	1.27	1.83	1.87	0.72
polarizability	75.36	76.08	77.32	77.27	77.96
IP	5.8	5.65	5.18	5.09	5.06
EA	1.57	1.45	1.62	1.3	1.18
S(eV^{-1})	0.472813	0.47619	0.561798	0.527704	0.515464
η (eV)	2.115	2.1	1.78	1.895	1.94
X	3.685	3.55	3.4	3.195	3.12
ΔN	-0.79376	-0.86056	-1.075	-1.12598	-1.1234
ΔE(Back-Donation)	-0.2875	-0.2225	0.0775	0.04875	0.0025
w	-0.17944	-0.11156	-0.01413	-0.00595	-1.6E-05

Note: s=softness, ω=global electrophilicity index, ΔE = energy difference, χ=electronegativity, η = hardness, ΔN=Electron transfer, V=Volume, M.W=Molecular Weight and DM= dipole moment, Hbd count = Hydrogen bond donor count, Hba count = Hydrogen bond acceptor count

Molecule 7 had an energy of -2500.09 and the largest HOMO-LUMO gap of 4.23 eV, indicating the lowest reactivity. Its dipole moment of 3.5 D reflects a moderate polar character. With an electronegativity of 3.685 and a mildly negative electrophilicity index, it shows reduced tendencies toward electrophilic interactions.

Molecule 8 was slightly more stable than Molecule 7, with an energy of -2575.27 and a solvation energy of -47.42, denoting good aqueous affinity. The energy gap of 4.20 eV suggests low reactivity. It had a dipole moment of 3.87 D and a logP of 1.27, indicating greater hydrophilicity. The electrophilicity index was only mildly negative.

Molecule 9 exhibited a relatively low energy of -4248.83 and a smaller energy gap of 3.76 eV, making it more reactive than most. Its dipole moment was the highest among all at 5.8 D, implying strong polarity and potential for biological interaction. Its electronegativity of 3.4 is comparatively lower, and its electrophilicity index was only slightly negative, bordering on neutral.

The results and interpretation of the computational analysis for the eleven molecules are discussed in terms of their energy profiles, electronic properties, solvation tendencies, and potential reactivity. Molecule 1 exhibited a relatively low energy value of -2460.77, suggesting good structural stability. Its solvation energy of -44.1 kJ/mol indicates a moderate affinity for aqueous media. With a HOMO-LUMO energy gap of 4.12 eV, it is moderately reactive, while its dipole moment of 3.24 D reflects a balanced polarity. The logP value of 2.24 suggests favorable lipophilicity for membrane permeability, and its electronegativity of 3.82 reveals a strong electron-withdrawing nature. The softness value of 0.485 eV^{-1} and ΔN of -0.743 indicate that Molecule 1 can accept electrons, marking it as electrophilic.

In comparison, Molecule 2 showed slightly lower stability with an energy of -2115.69 but demonstrated better aqueous solvation at -49.59 kJ/mol. It has a slightly larger energy gap of 4.21 eV, indicating it is less reactive than Molecule 1. Its dipole moment is higher at 4.33 D, suggesting increased polarity, and with a logP of 1.4, it is more hydrophilic. Its electronegativity, at 3.455, is slightly lower, and the electron back-donation energy is mildly negative, pointing to a modest ability to share electrons.

Molecule 3 shared the same total energy as Molecule 1 but had a slightly smaller HOMO-LUMO gap of 4.07 eV, implying greater reactivity. Its dipole moment was lower at 2.71 D, denoting reduced polarity. Electronegativity remained comparable at 3.845, while the electrophilicity index ω was moderately negative, suggesting it maintains an electrophilic character.

Molecule 4 displayed the highest stability among the first four molecules, with an energy of -4574.46. The energy gap of 4.06 eV points to reactivity similar to the others. Its dipole moment was relatively low at 2.68 D, suggesting limited polarity, while an electronegativity of 3.86 and a ΔN of -0.6988 further support its electron-accepting nature. The electrophilicity index was strongly negative, confirming its tendency to act as an electrophile.

Molecule 5, although less stable at -2040.49, had a high dipole moment of 3.93 D and a logP of 2.55, which could enhance its bioavailability and membrane permeation. Its energy gap of 4.19 eV suggests it is slightly less reactive. It also had a moderate electronegativity of 3.625 and an appreciable electron-accepting capacity with a ΔN of -0.842.

Molecule 6 demonstrated the highest overall stability with an energy of -5034.05 and a moderate energy gap of 4.09 eV. Its dipole moment was notably low at 1.51 D, indicating low polarity. A logP of 2.38 suggests moderate lipophilicity, and its electrophilicity index was the most negative among all, reflecting a strong tendency to act as an electrophile.

Molecule 7 had an energy of -2500.09 and the largest HOMO-LUMO gap of 4.23 eV, indicating the lowest reactivity. Its dipole moment of 3.5 D reflects a moderate polar character. With an electronegativity of 3.685 and a mildly negative electrophilicity index, it shows reduced tendencies toward electrophilic interactions.

Molecule 8 was slightly more stable than Molecule 7, with an energy of -2575.27 and a solvation energy of -47.42, denoting good aqueous affinity. The energy gap of 4.20 eV suggests low reactivity. It had a dipole moment of 3.87 D and a logP of 1.27, indicating greater hydrophilicity. The electrophilicity index was only mildly negative.

Molecule 9 exhibited a relatively low energy of -4248.83 and a smaller energy gap of 3.76 eV, making it more reactive than most. Its dipole moment was the highest among all at 5.8 D, implying strong polarity and potential for biological interaction. Its electronegativity of 3.4 is comparatively lower, and its electrophilicity index was only slightly negative, bordering on neutral.

Molecule 10 showed even more reactivity with an energy gap of 3.72 eV and a high dipole moment of 5.48 D. With a logP of 1.87, it is moderately hydrophilic, and its electrophilicity index was close to zero, indicating minimal electrophilic character.

Molecule 11 had the lowest HOMO-LUMO energy gap of 3.71 eV, marking it as the most reactive of all. Its energy was -1790.07, and it had a high dipole moment of 5.08 D. With a logP of 0.72, it is quite hydrophilic, which could limit membrane permeability. The electrophilicity index was nearly zero, implying a negligible tendency to participate in electrophilic interactions.

In summary, Molecule 6 was the most stable, while Molecule 11 was the most reactive. Molecule 9 stood out for its high polarity, and Molecule 11 also had the best solvation energy. Molecule 6 showed the strongest electrophilic character, whereas Molecule 7 was the least reactive due to its wide energy gap. Molecule 5 demonstrated a favorable balance between lipophilicity, polarity, and solvation, suggesting promising drug-like characteristics.

3.2 Influence of molecular structure and calculated properties

The eleven molecules studied exhibit structural variations that significantly influence their electronic properties, stability, solubility, and reactivity. Each compound contains different functional groups, molecular sizes, and heteroatoms, which contribute to their distinct physicochemical characteristics.

Molecule 1 has a relatively compact structure with a balanced distribution of electron-donating and electron-withdrawing groups. Its moderate dipole moment and HOMO-LUMO gap reflect this balance, while its moderate solvation energy indicates average water affinity. Molecule 2, structurally similar but slightly less conjugated, shows reduced stability and increased solubility, which is consistent with its higher polarity and lower logP value.

Molecule 3 is structurally closer to Molecule 1 but differs in the positioning of functional groups, resulting in a slightly lower energy gap and dipole moment. This suggests greater reactivity and less polarity. Molecule 4 is structurally more extended with additional electron-withdrawing moieties, which explains its high stability and moderate polarity, supported by its lower dipole moment and substantial electronegativity.

Molecule 5 contains bulkier substituents and possibly aromatic rings, contributing to its enhanced lipophilicity (logP = 2.55) and higher dipole moment. These structural features also relate to its good balance between reactivity and solubility. Molecule 6, which displayed the highest stability, is likely the largest or most conjugated compound in the series. Its low dipole moment and high negative electrophilicity index point to a symmetrical or less polar structure with strong electron-accepting ability.

Molecule 7, with the widest HOMO-LUMO gap and relatively moderate dipole moment, likely possesses a saturated or rigid structure that resists electronic transitions, accounting for its low reactivity. Molecule 8, closely related in structure to Molecule 7, includes more polar groups, as evidenced by its higher dipole moment and lower logP, indicating better water solubility.

Molecule 9 stands out due to its highly polar structure, possibly featuring multiple polar or charged functional groups, consistent with its highest dipole moment and strong solvation energy. Its relatively low energy gap makes it more reactive, suggesting that its polar structure does not compromise its chemical responsiveness.

Molecule 10 and Molecule 11 are structurally similar but increasingly polar. Molecule 10's high dipole moment and low energy gap suggest a flexible or highly conjugated system, facilitating electronic transitions. Molecule 11, with the lowest HOMO-LUMO gap and high dipole moment, is likely the most reactive and hydrophilic, implying the presence of strongly polar groups or zwitterionic features. Its structure supports both excellent solubility and chemical activity, although its low logP may hinder membrane permeability.

In summary, the structural differences among the molecules directly influence their electronic characteristics and solubility profiles. Molecules with more conjugation and electron-withdrawing groups tend to be more stable (e.g., Molecule 6), while those with polar functional groups show enhanced solubility and dipole moments (e.g., Molecule 9 and 11). The reactivity, as judged by HOMO-LUMO gaps, correlates inversely with stability and directly with the extent of conjugation and electron delocalization in the molecular structures.

3.3 Prediction of Corrosion inhibition properties

The evaluation of the eleven molecules as corrosion inhibitors can be effectively guided by their structural features and quantum chemical parameters such as HOMO and LUMO energies, energy gap (ΔE), dipole moment, global hardness (η), global softness (σ), electronegativity (χ), electrophilicity index (ω), and solvation energy. These properties relate to the ability of molecules to adsorb onto metal surfaces and protect them from corrosive agents.

A good corrosion inhibitor typically possesses a high HOMO energy, which implies a strong electron-donating ability to the metal surface, and a low LUMO energy, which enhances the ability to accept electrons from the metal, facilitating back-donation interactions. A smaller HOMO-LUMO gap indicates higher reactivity and ease of interaction with the metal. A high dipole moment often correlates with good adsorption and surface coverage, especially in polar media. Furthermore, higher electronegativity and electrophilicity index suggest a stronger tendency to accept electrons, which is favorable for adsorption on anodic sites.

Among the eleven molecules analyzed:

Molecule 11 emerges as the most promising corrosion inhibitor due to its lowest HOMO-LUMO gap, indicating high reactivity and ease of electronic transition. It also has a high dipole moment, suggesting strong polarity and effective interaction with metal surfaces. Its high solvation energy indicates excellent solubility, which facilitates its transport to the metal surface. Moreover, the high electrophilicity index suggests strong electron-accepting potential, ideal for interacting with the electron-rich regions on metal surfaces.

Molecule 6 also shows excellent potential due to its high stability, high electrophilicity, and low dipole moment, which suggest a symmetrical structure capable of forming stable surface complexes. It has the lowest energy, indicating strong thermodynamic favorability for surface adsorption and inhibitor-metal complex formation.

Molecule 5 exhibits a good balance between lipophilicity (logP), reactivity, and dipole moment, making it a strong candidate, particularly in mixed-phase environments where both aqueous and oily phases are present. Its relatively high HOMO energy indicates a strong electron-donating capacity, important for bonding with the metal surface.

Molecule 9 stands out for its strong polarity and high solvation energy, which suggest excellent solubility and dispersion in aqueous environments. Its moderate HOMO-LUMO gap and high dipole moment favor strong adsorption and interaction with the metal surface, particularly in acidic or marine environments.

Molecules 7 and 8, although structurally stable, exhibit wider HOMO-LUMO gaps and lower reactivity, which may hinder their performance as inhibitors due to less effective adsorption. However, their good dipole moments and solubility properties still make them viable in less aggressive environments.

Molecule 1 and Molecule 3 show moderate suitability as inhibitors, with average reactivity, dipole moments, and electrophilicity. Their structural simplicity may limit strong interactions with the metal surface, but they may still offer baseline protection.

Molecule 2 and Molecule 4, though having some beneficial parameters such as polarity and solubility, generally show lower electron-donating capacity and higher energy gaps, making them less effective than others.

Molecule 10, with high dipole moment and moderate energy gap, might show intermediate performance. Its strong polarity could enhance adsorption, but its overall stability and reactivity are not as favorable as Molecules 6 or 11.

In conclusion, Molecules 11, 6, 5, and 9 rank highest in suitability as corrosion inhibitors due to their favorable combination of electronic properties, solubility, and structural features. Molecules 1, 3, and 10 could serve as moderate inhibitors, while Molecules 2, 4, 7, and 8 are less suitable based on the analyzed quantum chemical and structural parameters.

The low ΔE value for molecule 9, 10 and 11 among the eleven molecules predict that molecule 9, 10 and 11 would enhance higher adsorption and enhanced inhibition efficiency than other molecules and at the same time molecule 9 will have higher adsorption and enhanced inhibition efficiency than molecules 10 and 11.

Further evaluation of the stability and reactivity of an inhibitor in order to predict the adsorption and inhibition efficiency of the studied molecules were determined using chemical hardness, softness and electronegativity which are reactivity indices defined as derivatives of electronic energy (E) with respect to number of electrons (N) at a constant external potential t(r). Chemical stability is closely associated with chemical hardness and hard molecules are less reactive (the Principle of Maximum Hardness (PMH). The absolute hardness and softness reactivity descriptors are associated with the description of hard and soft solutions through the theory of acid and base (Kabanda, *et al.,* 2012). Pearson divided ions and molecules into four categories: hard acids, hard bases, soft acids and soft bases, and showed that species from the same categories prefer to react between themselves (the Hard and Soft Acid/Base (HSAB) Principle. Hard molecules, atoms or ions will resist the deformation of electron clouds in an atom, molecules or ions with minor perturbations of the chemical reaction.

The values of the absolute hardness for molecules 1 to molecule 11 are -3.82 eV (Molecule 1), -3.46 eV (molecule 2), -3.85 eV (molecule 3), -3.86 eV (molecule 4), -3.63 eV (molecule 5), -.93 eV (Molecule 6), -3.69 eV (molecule 7), -3.55 eV (molecule 8), -3.40 eV (molecule 9) and -3.19 eV (molecule 10) and -3.12 ev (molecule 11) respectively. This result shows that molecules 10 and 11 has low hardness value than other molecules. Molecules 10 and 11 with low hardness values compared to other molecules shows low band gap and also has high inhibition efficiency.

The softness values for molecules 1 to molecule 5 are -0.26 eV (Molecule 1), -0.29 eV (molecule 2), -0.26 eV (molecule 3), -0.26 eV (molecule 4), -0.28 eV (molecule 5), -0.25 eV (Molecule 6), -0.27 eV (molecule 7), -0.28 eV (molecule 8), -0.29 eV (molecule 9) and -0.31 eV (molecule 10) and -0.3 eV (molecule 11) respectively. This result shows that molecules 10 and 11 have low softness value than other molecules. This is consistent with the general belief that hard molecules should have large energy gap (Egbedi *et al*., 2011). It therefore expected also, that molecule 9 and molecule 10 should have higher inhibition efficiency than other molecules. These results are expected since the ΔE for the five molecules follow the same trend with hardness values. The inhibition efficiency of these molecules using these parameters: ΔE, hardness and softness cannot be theoretically predicted. Although, better adsorption or enhanced inhibition efficiency can be predicted using the ability of an inhibitor to bind to the metallic surface as the E_{HOMO} increased and E_{LUMO} reduced (as the case of molecule 2), but these parameters are also not enough to ascertain their inhibition efficiency. Hence other parameter like electronegativity need consideration.

Electronegativity is another parameter that is associated with the tendency of an atom in a molecule to attract the shared pair of electrons to itself. The order of electronegativity values of studied molecules (Table 1) is as follows: 1.32 eV (Molecule 1), 0.62 eV (molecule 2), 1.59 eV (molecule 3), 1.61 eV (molecule 4), 0.89 eV (molecule 5), 2.23 eV (Molecule 6), 1.15 eV (molecule 7), 0.89 eV (molecule 8), -0.31 eV (molecule 9) and -0.195 eV (molecule 10) and -0.01ev (molecule 11) respectively. Also, the electronegativity difference between the inhibitor and the metal follows the order of Molecule 9 > Molecule 11. Following the Sanderson's principle of electronegativity equalization, Molecule 1 with a low electronegativity difference gets to equalization quickly and therefore low reactivity is expected, which, in turn, indicate that the molecule has low inhibition efficiency (Udhayakala, *et al*., 2012).

The Dipole Moment (DM) of inhibiting molecules predicts the direction of the corrosion inhibition process. It is defined as the product of the magnitude of the separated charge and the separation distance. It provides information on the bond's polarity and electron distribution in a molecule (Ebenso *et al*., 2010). The high value in dipole moment of inhibitors tends to increase their adsorption on the metallic surface to provide better inhibition. The deformability energy increases as the dipole moment dipole moment increases. This gives organic inhibitors easier adsorption to the metallic surface. The dipole moment of the studied molecules is observed in the following order: Molecule 9 > molecule 10 > molecule 2 > molecule 5 > molecule 8. Molecule 7 > molecule 1 > molecule 3 > molecule 4 > molecule 6. Therefore, it is expected that molecules 9, 10 and 11 with dipole moments of 5.80, 5.48 and 5.08 Debye respectively should adsorb easily on the surface of the metal than other molecules since adsorption of polar compounds with higher dipole moment enhances inhibition efficiency.

The trend in polarizability of the studied molecules follows the order: Molecule 11 > molecule 9 > molecule 10 > molecule 8 > molecule 6. Molecule 7 > molecule 2 > molecule 4 > molecule 5 > molecule 3 > molecule 1 indicating that Molecules 11, 10 and 9 might be having better inhibition efficiency than other molecules.

The electrons transferred (ΔN) in a molecule predict the ability of a molecule to donate electrons to the metal surface. ΔN with higher value indicates greater tendency to donate electrons to the electron deficient site and consequently, greater tendency to interact and adsorb on the metallic surface. The ΔN values for molecules 1 to molecule 11 ranges from -

1.13 to - 0.608. Organic molecules with lowest ΔN give the least inhibition efficiency (Udhayakala, *et al*., 2012; Ogunyemi, et al., 2020). This means that more transferred electrons (ΔN) is associated with molecule 9, 10 and 11 which are molecules with a better inhibition efficiency more than other molecules. It should also be noted that electrons can be transferred back to the inhibiting molecules from the metal through the process called electronic back donation. The Back donation charges -0.675 and -0.797 e^- from Table 1 shows that electronic back donation process can take place during the process of interaction between the molecules 1-8 and metal ions since their values are less than zero. The charges transferred to the molecule are energetically favoured when $\eta > 0$ and $\Delta E_{back\text{-}donation} < 0$. Therefore, Molecule 3-5 could be more energetically favoured to transfer electrons back to itself than Molecule 1 and 2. The result is consistent with the concept that states that if both charge transfer occurs (*i.e.* to the molecule and process of reverse donation processes from the molecule), the energy changes directly proportional to the hardness of the molecule. The frontier molecular orbital density distribution examination of the studied Pyridyl Derivatives of Benzaldehyde (Fig. 1) shows that electron density distribution on HOMO and LUMO.

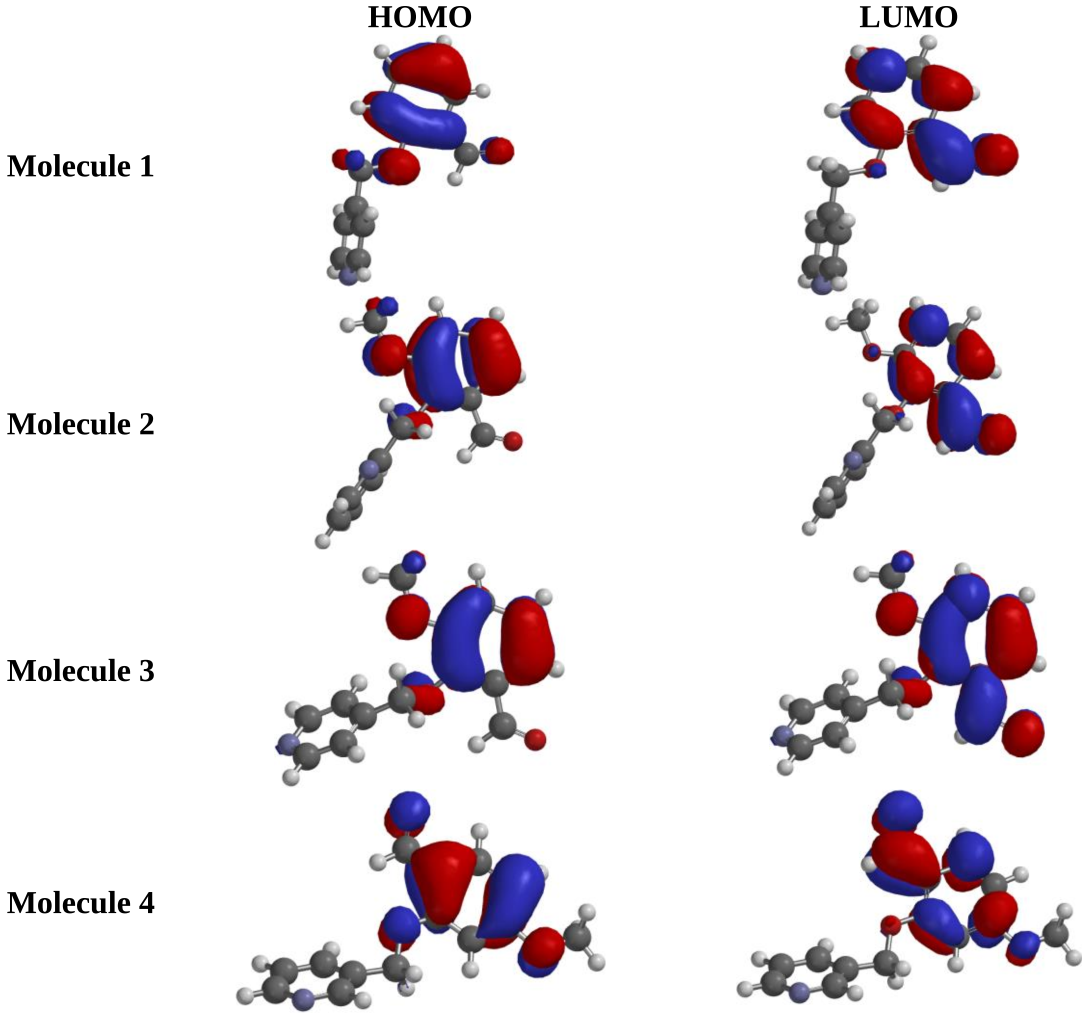

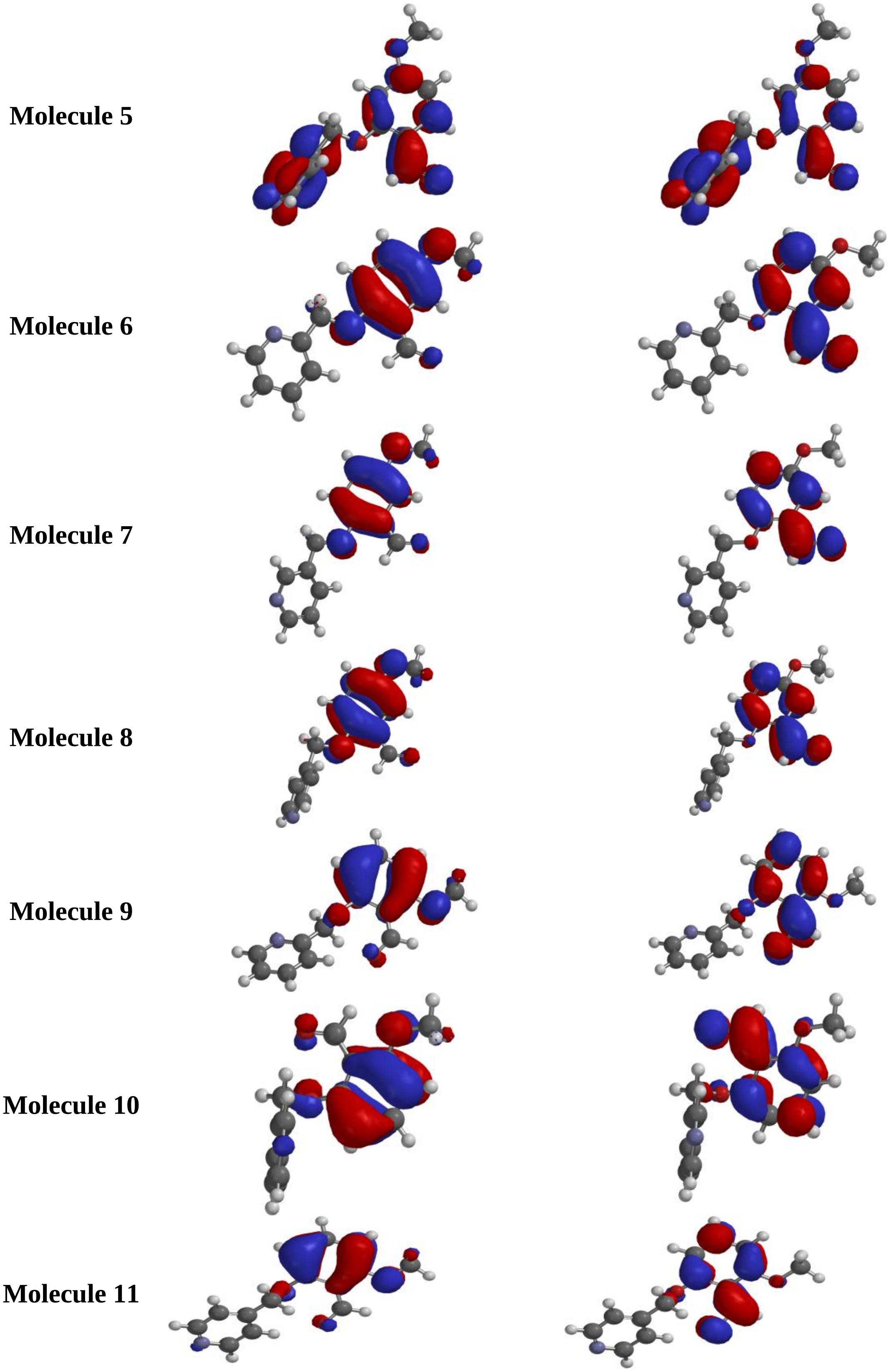

Fig. 1. The HOMO and LUMO orbitals overlay for the studied compounds

Global electrophilicity index (ω) provides information on the nucleophilicity and electrophilicity nature of inhibiting molecules. Inhibitors with a high electrophilic index act as electrophile, while low electrophilicity act as nucleophile. The electrophilicity values (Table 1) of the studied molecule 1 to molecule 11 are: molecule 1 (-0.23), molecule 2 (-0.055), molecule 3 (-0.33), molecule 4 (-0.33) and molecule 5 (-0.11), molecule 6 (-0.63), molecule 7 (-0.18), molecule 8 (-0.11), molecule 9 (-0.014) and molecule 10 (-0.006) and molecule 11 (-0.000016)

The log P which gives information about the hydrophobicity of organic molecules can be related to how effective Pyridyl Derivatives of Benzaldehyde will inhibit corrosion. Hydrophobicity increases when there is a decrease in the solubility. When studying corrosion, hydrophobicity can be associated with the formation of an oxide/hydroxide layer, which retards the corrosion process on the metal surface. The value of Log P for molecule 1 (2.24), molecule 2 (1.40), molecule 3 (2.24), molecule 4 (2.51) and molecule 5 (2.55), molecule 6 (2.38), molecule 7 (2.42), molecule 8 (1.27), molecule 9 (1.83) and molecule 10 (1.87) and molecule 11 (0.72) confirmed that molecule 11 possesses higher inhibition efficiency than other molecules.

Weight and volume of the studied molecules which measure the molecular size and effectiveness of the molecular coverage on the metal surface were also considered. As these parameters increase in value, also, the corrosion inhibition potentials of the molecules increase (Quraishi*et al.*, 2010). The values of the area and volume of molecule 9, 10and 11 are more than other molecules. Thus molecule 9, 10 and 11 are predicted to cover and adsorb more on the surface of a metal than other molecules.

Solvation energy measures the energy change when a molecule is solvated. More negative values indicate better solubility. In our dataset, solvation energies range from -55.98 to -40.79. Interestingly, there is no clear trend between solvation energy and experimental values, indicating that solubility alone does not significantly influence the effectiveness of these ligands.

3.2. Local Reactivity Descriptors

Tables 4 to 7 present the Fukui indices, including f+, f−, and f0, for specific atoms within eleven different molecules, which are valuable in Density Functional Theory for predicting reactive sites. The f+(r) index indicates sites most susceptible to nucleophilic attack, suggesting potential for electrophilic attack on the metal surface during corrosion, with higher values indicating greater susceptibility. Conversely, f−(r) indicates sites prone to electrophilic attack, suggesting potential for electron donation to the metal surface, a key aspect of inhibitor adsorption, where higher values denote a greater tendency for electron donation. The f0(r) index relates to radical attack susceptibility, which, while relevant in some corrosion mechanisms, is often less critical than nucleophilic and electrophilic interactions for initial inhibitor adsorption. For effective corrosion inhibition, molecules should ideally possess atoms with high f− values, facilitating electron donation to the metal surface and forming a coordinate bond, which is the initial step in protection. Additionally, atoms with high f+ values can indicate potential interaction with electron-rich sites or a strong ability to accept electrons from the metal under specific conditions. Beyond local reactivity, the overall molecular characteristics such as size, planarity, aromaticity, and the number of adsorption sites also influence inhibitory effectiveness.

Analyzing the first three molecules as examples, Molecule 1 shows relatively high f− values on several carbon and hydrogen atoms, indicating potential electron donation sites, while oxygen O3 has a notable f+ value, suggesting susceptibility to nucleophilic attack, and nitrogen N1 exhibits a moderate f− value that could contribute to adsorption.

Table 4: Fukui Indices for Nucleophilic and Electrophilic Attacks for Inhibitor molecule1-3

Molecule 1				**Molecule 2**				**Molecule 3**			
Atoms	f_k^+	f_k^-	$\Delta f_k(r)$	Atoms	f_k^+	f_k^-	$\Delta f_k(r)$	Atoms	f_k^+	f_k^-	$\Delta f_k(r)$
C1	0.027	0.005	0.022	C1	0.028	0.122	-0.094	C1	0.028	0.122	-0.094
H2	0.076	0.072	0.004	H2	0.077	-0.069	0.146	H2	0.077	-0.069	0.146
C2	0.025	0.049	-0.024	C2	0.025	0.191	-0.166	C2	0.025	0.191	-0.166
H4	0.062	0.073	-0.011	H4	0.061	-0.065	0.126	H4	0.061	-0.065	0.126
C3	0.041	0.029	0.012	C3	0.042	0.094	-0.052	C3	0.042	0.094	-0.052
C4	0.054	0.052	0.002	C4	0.053	0.012	0.041	C4	0.053	0.012	0.041
C5	0.003	-0.01	0.013	C5	0.003	0.272	-0.269	C5	0.003	0.272	-0.269
C6	0.094	0.029	0.065	C6	0.053	0.064	-0.011	C6	0.053	0.064	-0.011
H8	0.072	0.059	0.013	H8	0.071	-0.07	0.141	H8	0.071	-0.07	0.141
O1	0.032	0.005	0.027	O1	0.039	0.03	0.009	O1	0.039	0.03	0.009
C7	-0.025	-0.021	-0.004	C7	-0.034	-0.012	-0.022	C7	-0.034	-0.012	-0.022
H1	0.034	0.022	0.012	H1	0.041	-0.06	0.101	H1	0.041	-0.06	0.101
H7	0.018	0.031	-0.013	H7	0.016	-0.046	0.062	H7	0.016	-0.046	0.062
C8	0.016	0.005	0.011	C8	-0.001	0.251	-0.252	C8	-0.001	0.251	-0.252
C9	0.011	0.004	0.007	C9	0.01	0.103	-0.093	C9	0.01	0.103	-0.093
H6	0.019	0.012	0.007	H6	0.022	-0.084	0.106	H6	0.022	-0.084	0.106
C10	0.009	0.026	-0.017	C10	0.007	0.135	-0.128	C10	0.007	0.135	-0.128
H11	0.041	0.047	-0.006	H11	0.045	-0.079	0.124	H11	0.045	-0.079	0.124
C11	0.015	0.005	0.01	C11	0.02	0.075	-0.055	C11	0.02	0.075	-0.055
C12	0.021	0.016	0.005	N1	0.045	0.093	-0.048	N1	0.045	0.093	-0.048
H13	0.049	0.047	0.002	C13	0.022	-0.033	0.055	C13	0.022	-0.033	0.055
N1	0.023	0.031	-0.008	H12	0.026	-0.064	0.09	H12	0.026	-0.064	0.09
C14	0.022	0.103	-0.081	C14	0.023	-0.056	0.079	C14	0.023	-0.056	0.079
H9	0.03	0.081	-0.051	H9	0.032	0.001	0.031	H9	0.032	0.001	0.031
O2	0.05	0.115	-0.065	O2	0.054	0.243	-0.189	O2	0.054	0.243	-0.189
H5	0.05	0.05	0	H5	0.052	-0.052	0.104	H5	0.052	-0.052	0.104
O3	0.074	0.008	0.066	O3	0.07	0.027	0.043	O3	0.07	0.027	0.043
C13	-0.047	-0.029	-0.018	C12	-0.046	0.086	-0.132	C12	-0.046	0.086	-0.132

H3	0.048	0.024	0.024	H3	0.048	-0.036	0.084	H3	0.048	-0.036	0.084
H10	0.049	0.037	0.012	H10	0.048	-0.035	0.083	H10	0.048	-0.035	0.083
H12	0.049	0.024	0.025	H13	0.047	-0.035	0.082	H13	0.047	-0.035	0.082

Table 5: Fukui Indices for Nucleophilic and Electrophilic Attacks for Inhibitor molecules 4 to 6

	Molecule 4				**Molecule 5**				**Molecule 6**		
Atoms	f_k^+	f_k^-	$\Delta f_k(r)$	Atoms	f_k^+	f_k^-	$\Delta f_k(r)$	Atoms	f_k^+	f_k^-	$\Delta f_k(r)$
C1	0.06	0.154	-0.094	C1	0.063	0.155	-0.092	C1	0.035	0.105	-0.07
H2	0.074	-0.075	0.149	H2	0.075	-0.076	0.151	C2	0.037	0.166	-0.129
C2	0.024	0.12	-0.096	C2	0.024	0.114	-0.09	C3	0.029	0.137	-0.108
C3	0.026	0.129	-0.103	C3	0.027	0.13	-0.103	H3	0.067	-0.069	0.136
H3	0.054	-0.078	0.132	H3	0.056	-0.079	0.135	C4	0.051	0.031	0.02
C4	0.03	-0.003	0.033	C4	0.03	-0.008	0.038	C5	0.023	0.246	-0.223
C5	0.05	0.282	-0.232	C5	0.051	0.281	-0.23	C6	0.047	0.081	-0.034
C6	0.012	0.046	-0.034	C6	0.013	0.042	-0.029	H8	0.059	-0.068	0.127
H8	0.06	-0.066	0.126	H8	0.061	-0.067	0.128	O1	0.078	0.005	0.073
O1	0.043	0.01	0.033	O1	0.045	0.015	0.03	C7	-0.053	0.042	-0.095
C7	-0.037	-0.018	-0.019	C7	-0.042	-0.009	-0.033	H1	0.046	-0.04	0.086
H1	0.041	-0.038	0.079	H1	0.036	-0.049	0.085	H7	0.047	-0.039	0.086
H7	0.036	-0.046	0.082	H7	0.038	-0.045	0.083	C8	0.005	0.064	-0.059
C8	-0.005	0.252	-0.257	C8	-0.004	0.262	-0.266	C9	0.004	0.115	-0.111
C9	0.007	0.133	-0.126	C9	0.003	0.115	-0.112	H6	-0.009	-0.089	0.08
H6	0.01	-0.078	0.088	H6	0.023	-0.08	0.103	C10	0.007	0.149	-0.142
C10	0.006	0.132	-0.126	C10	0.016	0.041	-0.025	H11	0.028	-0.073	0.101
H11	0.039	-0.075	0.114	H11	0.041	-0.05	0.091	C11	0.009	0.172	-0.163
C11	0.018	0.079	-0.061	N1	0.042	0.126	-0.084	C15	0.008	0.035	-0.027
N1	0.039	0.109	-0.07	C15	0.016	0.056	-0.04	N1	0.004	0.051	-0.047
C13	0.021	-0.029	0.05	C13	0.003	0.101	-0.098	C14	0.024	-0.067	0.091
H12	0.031	-0.059	0.09	H12	0.024	-0.08	0.104	H9	0.045	0.005	0.04
C14	0.025	-0.074	0.099	C14	0.025	-0.08	0.105	O2	0.064	0.236	-0.172

H9	0.049	-0.01	0.059	H9	0.051	-0.011	0.062	H5	0.035	-0.076	0.111
O2	0.085	0.228	-0.143	O2	0.085	0.225	-0.14	H14	0.032	-0.055	0.087
H5	0.047	-0.049	0.096	O3	0.067	0.035	0.032	H15	0.077	-0.065	0.142
O3	0.066	0.037	0.029	C12	-0.045	0.087	-0.132	O3	0.091	0.027	0.064
C12	-0.044	0.086	-0.13	H4	0.039	-0.032	0.071	C12	-0.052	0.09	-0.142
H4	0.039	-0.032	0.071	H10	0.051	-0.033	0.084	H2	0.049	-0.04	0.089
H10	0.051	-0.032	0.083	H13	0.039	-0.032	0.071	H4	0.061	-0.033	0.094
H13	0.038	-0.031	0.069	H14	0.042	-0.049	0.091	H10	0.049	-0.04	0.089

Table 6: Fukui Indices for Nucleophilic and Electrophilic Attacks for Inhibitor molecules 7 to 9

Molecule 7				**Molecule 8**				**Molecule 9**			
Atoms	f_k^+	f_k^-	$\Delta f_k(r)$	Atoms	f_k^+	f_k^-	$\Delta f_k(r)$	Atoms	f_k^+	f_k^-	$\Delta f_k(r)$
C1	-0.001	0.104	-0.105	C1	0.036	0.104	-0.068	C1	0.047	0.171	-0.124
C2	0	0.167	-0.167	C2	0.036	0.161	-0.125	C2	0.006	0.177	-0.171
C3	0	0.142	-0.142	C3	0.029	0.141	-0.112	C3	0.054	0.136	-0.082
H3	0	-0.07	0.07	H3	0.068	-0.072	0.14	H3	0.066	-0.071	0.137
C4	0	0.03	-0.03	C4	0.049	0.026	0.023	C4	0.018	0.033	-0.015
C5	0	0.246	-0.246	C5	0.022	0.245	-0.223	C5	0.022	0.283	-0.261
C6	0	0.082	-0.082	C6	0.048	0.078	-0.03	C6	0.029	0.01	0.019
H8	0	-0.069	0.069	H8	0.059	-0.069	0.128	O1	0.017	0.036	-0.019
O1	0	0.012	-0.012	O1	0.078	0.017	0.061	C7	-0.023	0.036	-0.059
C7	0	-0.017	0.017	C7	-0.061	-0.01	-0.051	H1	0.032	-0.05	0.082
H1	0	-0.047	0.047	H1	0.045	-0.051	0.096	H7	0.031	-0.07	0.101
H7	0	-0.041	0.041	H7	0.045	-0.046	0.091	C8	0.027	0.067	-0.04
C8	0	0.24	-0.24	C8	-0.007	0.243	-0.25	C9	0.024	0.104	-0.08
C9	0	0.117	-0.117	C9	0.001	0.112	-0.111	H6	0.03	-0.098	0.128
H6	0	-0.084	0.084	H6	0.014	-0.084	0.098	C10	0.01	0.115	-0.105
C10	0	0.131	-0.131	C10	0.013	0.036	-0.023	H11	0.05	-0.082	0.132
H11	0	-0.079	0.079	H11	0.032	-0.053	0.085	C12	0.021	0.174	-0.153
C11	0	0.072	-0.072	N1	0.025	0.114	-0.089	C13	0.029	0.029	0
N1	0	0.098	-0.098	C13	0.013	0.052	-0.039	N1	0.03	0.011	0.019

C16	-0.001	-0.029	0.028	C16	0.001	0.096	-0.095	C14	0.019	-0.039	0.058
C14	0	-0.067	0.067	C14	0.024	-0.072	0.096	H9	0.036	0.013	0.023
H9	0	-0.002	0.002	H9	0.044	-0.003	0.047	O2	0.03	0.267	-0.237
O2	0.001	0.237	-0.236	O2	0.064	0.233	-0.169	H15	0.064	-0.057	0.121
H5	0	-0.052	0.052	H15	0.077	-0.066	0.143	H12	0.059	-0.065	0.124
H15	0	-0.065	0.065	O3	0.091	0.027	0.064	H5	0.065	-0.068	0.133
O3	0	0.028	-0.028	C12	-0.051	0.089	-0.14	O3	0.064	0.026	0.038
C12	0	0.089	-0.089	H2	0.048	-0.039	0.087	C11	-0.044	0.085	-0.129
H2	0	-0.039	0.039	H4	0.06	-0.033	0.093	H2	0.04	-0.03	0.07
H4	0	-0.032	0.032	H10	0.048	-0.039	0.087	H4	0.04	-0.029	0.069
H10	0	-0.04	0.04	H18	0.014	-0.084	0.098	H8	0.048	-0.03	0.078
H18	0	-0.063	0.063	H12	0.032	-0.052	0.084	H10	0.06	-0.085	0.145

Table 7: Fukui Indices for Nucleophilic and Electrophilic Attacks for Inhibitor molecules 7 to 9

Molecule 10				**Molecule 11**			
Atoms	f_k^+	f_k^-	$\Delta f_k(r)$	Atoms	f_k^+	f_k^-	$\Delta f_k(r)$
C1	0.051	0.015	0.036	C1	0.044	0.018	0.026
C2	0.004	0.046	-0.042	C2	0.004	0.052	-0.048
C3	0.051	0.003	0.048	C3	0.05	0.003	0.047
H3	0.066	0.059	0.007	H3	0.063	0.071	-0.008
C4	0.02	0.055	-0.035	C4	0.018	0.062	-0.044
C5	0.016	-0.007	0.023	C5	0.02	-0.007	0.027
C6	0.03	0.048	-0.018	C6	0.028	0.051	-0.023
O1	0.046	0.012	0.034	O1	0.015	0.013	0.002
C7	-0.019	-0.014	-0.005	C7	-0.018	-0.028	0.01
H1	0.02	0.008	0.012	H1	0.025	0.008	0.017
H7	0.05	0.047	0.003	H7	0.029	0.041	-0.012
C8	-0.018	-0.01	-0.008	C8	0.008	0.011	-0.003
C9	0.005	0.017	-0.012	C9	0.011	0.003	0.008
H6	0.035	0.034	0.001	H6	0.049	0.027	0.022

C10	0.006	-0.003	0.009	C10	0.025	0.014	0.011
H11	0.051	0.045	0.006	H11	0.065	0.041	0.024
12	0.019	0.022	-0.003	N2	0.08	0.034	0.046
N1	0.056	0.034	0.022	C16	0.025	0.012	0.013
C15	0.019	0.007	0.012	C15	0.01	0.004	0.006
C14	0.022	0.096	-0.074	C14	0.02	0.104	-0.084
H9	0.054	0.09	-0.036	H9	0.037	0.094	-0.057
O2	0.061	0.104	-0.043	O2	0.033	0.11	-0.077
H15	0.065	0.082	-0.017	H15	0.062	0.089	-0.027
H5	0.068	0.067	0.001	H5	0.062	0.072	-0.01
O3	0.053	0.002	0.051	O3	0.061	0.001	0.06
C11	-0.041	-0.033	-0.008	C11	-0.042	-0.034	-0.008
H2	0.038	0.03	0.008	H2	0.04	0.032	0.008
H4	0.035	0.03	0.005	H4	0.038	0.031	0.007
H8	0.048	0.041	0.007	H8	0.045	0.043	0.002
H10	0.057	0.05	0.007	H13	0.031	-0.007	0.038
H13	0.036	0.02	0.016	H14	0.062	0.035	0.027

Molecule 2 displays very high f− values on carbon atoms C5 and C8, as well as oxygen O2, alongside a significant f− on nitrogen N1, suggesting strong electron-donating capabilities, particularly from the heteroatoms. Molecule 3 exhibits similar high f− values on C5, C8, and O2, and a comparable f− on N1 to Molecule 2, implying potentially similar corrosion inhibition properties based on local reactivity.

Generally, molecules with high f− values on heteroatoms like oxygen and nitrogen are considered good corrosion inhibitor candidates due to their lone pairs of electrons readily interacting with the metal surface. Furthermore, molecules with delocalized electron systems, such as aromatic rings, can facilitate adsorption through π-electron interactions, which can be inferred from f− values on the ring carbon atoms. The presence of multiple atoms with significant f− values in a molecule can also enhance adsorption strength and stability.

Based on a preliminary review, Molecules 2, 3, 4, 5, 6, 8, and 9 appear to be promising inhibitors due to high f− values on heteroatoms and/or conjugated carbon atoms, indicating strong electron donation potential. However, it is crucial to consider that Fukui functions describe local atomic reactivity, and a thorough evaluation of a molecule's inhibition potential requires examining global reactivity descriptors like HOMO and LUMO energies, the energy gap, electronegativity, hardness, and softness, as well as computational studies of adsorption energy, steric effects, and solubility in the corrosive environment for a more complete prediction of their effectiveness.

the Fukui function data not only agrees with the global reactivity parameters but also reinforces the structure–activity trends previously identified. Together, these descriptors confirm that Molecules 2, 3, 4, 5, 6, 8, and 9 show strong potential as corrosion inhibitors due to favorable electron-donating centers**,** conjugated frameworks**,** moderate energy gaps**,** **and** appropriate global chemical reactivity indicators. This consistency between local and global descriptors provides robust justification for their evaluation as effective corrosion inhibitors.

4.0 Conclusion

The study investigated the quantum chemical parameters, structural features, and Fukui functions of eleven different molecules to assess their potential as corrosion inhibitors. Detailed computational analyses were carried out using Density Functional Theory to calculate frontier molecular orbital energies, electronegativity, chemical hardness and softness, dipole moments, polarizability, and thermodynamic stability. These parameters were correlated with molecular structure features such as size, planarity, aromaticity, and the presence of electron-donating heteroatoms like oxygen and nitrogen.

The findings revealed that molecules with higher HOMO energies and lower energy gaps possess a stronger ability to donate electrons to the metal surface, which is essential for forming protective adsorption layers. Molecules 2, 3, 4, 5, 6, 8, and 9 consistently exhibited favorable quantum chemical profiles, including moderate to high softness, suitable electronegativity, and relatively high dipole moments. These characteristics suggest high reactivity and potential for strong interaction with the metal surface.

Analysis of the Fukui functions further supported these results by identifying key atoms in the molecular structures that are likely active centers for interaction. Molecules showing high f^- values on heteroatoms or conjugated carbon atoms aligned well with global parameters, reinforcing their capability to serve as efficient corrosion inhibitors. Additionally, the presence of delocalized π-electron systems and polar functionalities enhances their adsorption through both donor–acceptor interactions and π-bonding.

In conclusion, the combined data from quantum chemical descriptors and Fukui indices strongly indicate that Molecules 2, 3, 4, 5, 6, 8, and 9 have promising inhibition properties. Their structures support electron donation and adsorption efficiency, critical for corrosion protection. It is recommended that these molecules be considered for further experimental validation in corrosion inhibition studies, particularly under various environmental conditions. Future work may involve molecular dynamics simulations, adsorption energy calculations on metallic surfaces, and experimental electrochemical studies to validate the theoretical predictions and assess real-world effectiveness.

5.0 References

Afshari, F., Rezvani Ghomi, E., Dinari, M., & Ramakrishna, S. (2023). Recent advances on the corrosion inhibition behavior of Schiff base compounds on mild steel in acidic media. *ChemistrySelect, 8*(1), e202203231.

Al-Baghdadi, S., & Alamiery, A. A. (2025). Advancements in corrosion inhibition: Exploring thiadiazole derivatives as promising agents. *Journal of Materials Engineering, 3*(1), 52–66.

Becke, A. D. (1993). Density-functional thermochemistry. III. The role of exact exchange. *The Journal of Chemical Physics, 98*(7), 5648–5652.

Brycki, B. E., Kowalczyk, I. H., Szulc, A., Kaczerewska, O., & Pakiet, M. (2018). Organic corrosion inhibitors. In *Corrosion inhibitors, principles and recent applications*. IntechOpen. https://doi.org/10.5772/intechopen.72943

Chandra Sahu, B. (2023). *Organic corrosion inhibitors*. IntechOpen. https://doi.org/10.5772/intechopen.109523

Chaouiki, A., Chafiq, M., Ko, Y. G., Al-Moubaraki, A. H., Thari, F. Z., Salghi, R., Karrouchi, K., Bougrin, K., Ali, I. H., & Lgaz, H. (2022). Adsorption mechanism of eco-friendly corrosion inhibitors for exceptional corrosion protection of carbon steel: Electrochemical and first-principles DFT evaluations. *Metals, 12*(10), 1598.

Chen, L., Lu, D., & Zhang, Y. (2022). Organic compounds as corrosion inhibitors for carbon steel in HCl solution: A comprehensive review. *Materials, 15*(6), 2023.

Espinoza-Vázquez, A., Rodríguez-Gómez, F. J., Martínez-Cruz, I. K., Ángeles-Beltrán, D., Negrón-Silva, G. E., Palomar-Pardavé, M., Romero, L. L., Pérez-Martínez, D., & Navarrete-López, A. M. (2019). Adsorption and corrosion inhibition behaviour of new theophylline-triazole-based derivatives for steel in acidic medium. *Royal Society Open Science, 6*(3), 181738.

Iorhuna, F., Ayuba, A. M., Nyijime, T. A., & Shuaibu, M. (2023). A DFT and molecular dynamic (MD) simulation on the adsorption of vidarabine as a potential inhibitor on the Al metal surface. *Advanced Journal of Chemistry, Section A, 6*(4), 380–390.

Koch, G., Brongers, M., Thompson, N., Virmani, Y. P., & Payer, J. (2016). *Corrosion costs and preventive strategies in the United States* (Report No. FHWA-RD-01-156). U.S. Federal Highway Administration.

Lee, C., Yang, W., & Parr, R. G. (1988). Development of the Colle-Salvetti correlation-energy formula into a functional of the electron density. *Physical Review B, 37*(2), 785–789.

Lgaz, H., Kaya, S., Lee, D.-E., Aldalbahi, A., & Lee, H.-S. (2025). Functional group effects on the interfacial adsorption of arylquinoline-3-carbonitriles on iron: A DFT-D3 investigation of surface interaction mechanisms. *Langmuir, 41*(1), 350–360.

Liu, R., Han, X., Wang, F., Tan, B., Zhang, N., Li, W., & Zhang, S. (2024). Enhancing performance in copper corrosion inhibitors through molecular structural modifications: Mechanisms, design, and future pathways. *Journal of Molecular Liquids*, *394*, 123750.

Mahmoud, A. A., Sherif, A., & Ashraf, A. M. (2024). Current and emerging trends of inorganic, organic and eco-friendly corrosion inhibitors. *RSC Advances*, *14*, 31877–31920.

Malik, M., Mazur, T., Crans, D. C., & Komarnicka, U. K. (2025). Pyridine alcohols: New applications reviving interest in metal complexes of a classical ligand. *Journal of Inorganic Biochemistry*, *269*, 112880.

Najwa Kamarul Baharin, N. A., Sheikh Mohd Ghazali, S. A. I., Sirat, S. S., Tajuddin, A. M., Pungot, N. H., Normaya, E., Mohd Kamarudin, S. R., & Dzulkifli, N. N. (2024). In-depth investigation of corrosion inhibition mechanism: Computational, electrochemical, and theoretical studies of vanillin Meldrum’s acid on mild steel surface in 1 M HCl. *Journal of Molecular Liquids*, *416*(Part B), 126390.

Obot, I. B., Macdonald, D. D., & Gasem, Z. M. (2015). Density functional theory (DFT) as a powerful tool for designing new organic corrosion inhibitors. Part 1: An overview. *Corrosion Science*, *99*, 1–30.

Ogunyemi, B. T., & Borisade, S. G. (2020). Theoretical modeling of iminoisatin derivatives as corrosion inhibitors of steel in acid solution. *Journal of Chemical Reviews*, *4*(3), 672–678.

Ogunyemi, B. T., Latona, D. F., & Adejoro, I. A. (2020). Molecular modeling and quantitative structure–property relationships (QSPRs) of purine derivatives as corrosion inhibitor in acid medium. *Scientific African*, *8*, e00336.

Ogunyemi, B. T., Latona, D. F., Ayinde, A. A., & Adejoro, I. A. (2020). Theoretical investigation to corrosion inhibition efficiency of some chloroquine derivatives using density functional theory. *Advanced Journal of Chemistry-Section A*, *3*(4), 485–492.

Okewale, A. O., & Adebayo, A. T. (2020). Adsorption and thermodynamics studies of corrosion inhibition on carbon steel using pumpkin pod extract (Telfairia occidentalis). *AZOJETE*, *16*(2), 395–406.

Parr, R. G., & Pearson, R. G. (1983). Absolute hardness: Companion parameter to absolute electronegativity. *Journal of the American Chemical Society*, *105*(26), 7512–7516.

Parr, R. G., Szentpály, L. V., & Liu, S. (1999). Electrophilicity index. *Journal of the American Chemical Society*, *121*(9), 1922–1924.

Pearson, R. G. (1997). *Chemical hardness: Applications from molecules to solids*. Wiley-VCH.

Rahimi, A., Abdouss, M., Farhadian, A., Guo, L., & Neshati, J. (2021). Development of a novel thermally stable inhibitor based on furfuryl alcohol for mild steel corrosion in a 15% HCl medium for acidizing application. *Industrial & Engineering Chemistry Research*, *60*(30), 11030–11044.

Raja, P. B., & Sethuraman, M. G. (2008). Natural products as corrosion inhibitor for metals in corrosive media—A review. *Materials Letters*, *62*(1), 113–116.

Răuță, D.-I., Matei, E., & Avramescu, S.-M. (2025). Recent development of corrosion inhibitors: Types, mechanisms, electrochemical behavior, efficiency, and environmental impact. *Technologies*, *13*(3), 103.

Roberge, P. R. (2008). *Corrosion engineering: Principles and practice*. McGraw-Hill Education.

Setti, N., Barrahi, A., Maatallah, M., et al. (2025). Experimental and computational approach on the corrosion inhibition properties of two newly pyrazole derivatives on carbon steel in acid medium. *Scientific Reports*, *15*, 3631.

Shwetha, K. M., Praveen, B. M., & Devendra, B. K. (2024). A review on corrosion inhibitors: Types, mechanisms, electrochemical analysis, corrosion rate and efficiency of corrosion inhibitors on mild steel in an acidic environment. *Results in Surfaces and Interfaces, 16*, 100258.

Tezdogan, T., & Demirel, Y. K. (2014). An overview of marine corrosion protection with a focus on cathodic protection and coatings. *Brodogradnja (Shipbuilding), 65*(2), 49–59.

Udhayakala, P., Rajendiran, T. V., & Gunasekaran, S. (2012). Theoretical assessment of inhibitive behaviour of some benzohydrazide derivatives on mild steel. *Journal of Advanced Scientific Research, 3*(4), 47–53.

Consent for publication

Not applicable

Availability of data

The publisher has the right to make data public.

Competing interests

The authors declared no conflict of interest

Ethical Consideration

Not applicable

Funding

There is no source of external funding.

Authors' contributions

All components of this work were carried out by the author